Modeling the Growth of Inflorescence

MengZhen Kang
LIAMA&NLPR, Institute of Automation
Chinese Academy of Sciences
Beijing, China
mzkang@nlpr.ia.ac.cn

Philippe de Reffye
Project DigiPlante
INRIA, Saclay
France
philippe.de_reffye@inria.fr

Ep Heuvelink
Horticultural Supply Chains
Wageningen University
Wageningen, the Netherlands
ep.heuvelink@wur.nl

Abstract

In many herbaceous plants with inflorescence, the axillary flowering branches remain in a substantial dormant stage between their initiation and the start of expansion. The durations of dormant stage, called growth delay, are linked to the positions of branches in plant architecture. For modeling biomass production and partitioning, it is essential to describe the growth delay to obtain the number of organs in expansion competing for the assimilates.

In this paper, position-dependent delay functions are proposed for herbaceous plants with different branching inflorescence. The delay intensities can change according to branch position or plant dynamic source-sink ratio, to simulate the apical dominance phenomena in plants with basipetal flowering sequences. Simulation results are given on the effect of delay parameters on plant architecture. By integrating the delay functions with GreenLab model, the growth process of chrysanthemum under two light levels were simulated. The current work provides a generic module for modeling the growth of individual organs in plants with inflorescence.

1. Introduction

An inflorescence is a cluster of flowers arranged on a stem that is composed of a main branch or a complicated arrangement of branches. In a deterministic inflorescence, there are several growth sequences of branches along a stem: basipetal (top-down), acropetal (bottom-up), and divergent (starting from the central part). Various combinations of inflorescence structures and flowering sequences are possible in plants. Many plants produce inflorescence, such as rapeseed, lettuce and chrysanthemum. When modeling the crop yield, in terms of either seed or flower production, simulation of the structure and growth sequence of inflorescence is an important issue.

Developmental models of inflorescence have been developed to simulate various inflorescence structures and flowering sequences [1][2]. The L-system based approach [1] was started by simulating the inflorescence in lettuce [3]; the flowering branches were initiated in top-down sequence to mimic the basipetal flowering sequence. Although visually realistic, botanically speaking, the top-down branch initiation contradict with the fact that the axillary meristems are formed earlier in older leaves than in younger leaves [4]. In some leafy inflorescence, for example the chrysanthemum, the branch leaves can occupy as high as 20% of total leaf biomass at the start of generative stage. If biomass is the main issue, the top-down initiation will bring systematic error by neglecting their contribution in biomass production and competition.

To properly simulate the development process of inflorescence, and to specify precisely the dynamics of the number of sink and source organs, growth delay has been introduced into plant growth model of chrysanthemum, which is the interval between the initiation and expansion of branch organs [5]. The growth delay is position-dependent. For example, in case of basipetal flowering, it takes more time for branches of lower position to start although they are initiated earlier than those of higher position. When growth delay is introduced, branch stems are initiated in parallel to main axis, but they have negligible sink strength until the start of expansion. In another application [6], the growth delay has been shown to be dependent on the ratio between assimilate supply and demand, or the dynamic source-sink ratio of plant [6]. This is inline with the observation on chrysanthemum, that at higher light level, more flowers can be produced at harvest stage [7]. However, in both previous works, the branching order was limited to one, which was insufficient to generalize.

In this paper, we propose a generic method for modeling the position-dependent growth delay in herbaceous plants of any branching order. Focus is given to the basipetal flowering sequence, which is very common in crops. The apical dominance phenomena were simulated by linking the delay intensity to the plant source-sink ratio. Simulation results are shown for effect of different delay functions on plant architecture. An example of application on chrysanthemum is shown to illustrate how the model can be calibrated and how it can be used for simulating the effect of the environment on plant growth.

978-0-7695-3988-1/10 $26.00 © 2010 IEEE
DOI 10.1109/PMA.2009.52

2. Method

Three sub-modules are necessary to simulate the development and expansion of herbaceous plants with inflorescence: (1) an organogenesis model for generating the topological structure; (2) a delay function describing the time duration from organ initiation (primordium) to organ expansion; (3) a functional model computing the biomass production and partitioning into plant structure, which gives the weights and sizes of organs. Combination of (1) and (2) generally leads to the so-called functional structure plant models [8]. The functional model can have different degrees of complexity, either based on simplified concepts as in GreenLab [6][9][10], or on more sophisticated processes as in [11]. Models contributing to part (1) and part (2) can be referred to other articles; here we focus on part (2), the delay function.

2.1. Locating a phytomer

To define a position-dependent growth delay function, the first task is to give the coordinate of each organ inside plant topological structure. For a herbaceous plant, the coordinate of a phytomer can be defined by $p+1$ integer numbers, p being the branching order of the axis. For example, for main stem, whose branching order is zero, an integer number i is sufficient to identify a phytomer of rank i from the stem base of plant. all organs inside a phytomer have the same coordinates. The coordinate of a branch is the same as that of phytomer where it is attached to. Therefore, branch (i) means a first-order branch located at phytomer (i). For a branching structure, the definition of the coordinate is recursive. For example, the phytomer of coordinate (i,j) indicates the j-th phytomer from the base of a first-order branch of coordinate i. Phytomer (i,j,k) indicates k-th phytomer from the base of a second-order branch of coordinate (i,j), etc. Fig. 1 shows a topological structure of four branching orders, where the coordinates of some phytomers are indicated. In the case of whorls, all the branches at the same position are supposed to have the same coordinate.

To define the plant topological structure, the (maximum) lengthes of each axis are given in the organogenesis model. For example, in Fig.1, the length of main stem is five phytomers, denoted as $T_1 = 5$. Let $T_2(i)$ be the length (number of phytomers) of the first-order branch located at abscissa i from base of main stem. In the example of Fig.1, $T_2(1) = 4$, $T_2(2) = 3$, *etc*. Similarly, let $T_3(i,j)$ be the length of the second-order branch of coordinate (i,j). Different recursive equations giving the lengthes of branches can be defined, leading to various topological structures. Following are several examples for the length of branches of first- and second- orders respectively. Such definition can be extended to higher-order branches.

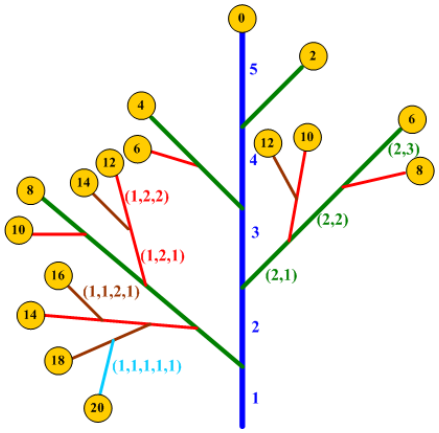

Figure 1. A inflorescence structure with four branching orders and basipetal flowering sequence. The structure is of self-similar property (see Eqn.4), with length of main stem $T_1 = 5$. Delay intensity is two (see Eqn.12). Numbers in ( ) indicates the coordinates of phytomers and branches. Each circle represents a terminal flower. The numbers in circles indicate the time (in cycle) from the initiation of the terminal phytomer of main stem to the expansion of current phytomer.

2.1.1. Constant branch length. In this case, a branch of a given order p have constant lengthes T_p^0 (Eqn.1), independent of its position. An drawing of such a topological stricture is shown in Fig.2(a).

$$T_2(i) = T_2^0; T_3(i,j) = T_3^0 \tag{1}$$

2.1.2. Increasing branch length until a maximum. The length of a branch may increase from the top of its bearing axis to the lower positions, until a maximum value T_p^0 is reached, see Fig.2(b).

$$T_2(i) = \begin{cases} T_1 - i, & i > T_1 - T_2^0, \\ T_2^0, & else \end{cases} \tag{2}$$

$$T_3(i,j) = \begin{cases} T_2(i) - j, & j > T_2(i) - T_3^0, \\ T_3^0, & else \end{cases} \tag{3}$$

2.1.3. Self-similar structure. If the length of a branch always increases from the top to the lower position of its bearing axis, it may lead to a self-similar structure, see Fig.2(c). If the branching order were infinite, the substructure would be always similar to its mother structure. The example in Fig.1 belongs to this type.

$$T_2(i) = T_1 - i; T_3(i,j) = T_2(i) - j \tag{4}$$

2.1.4. Self-similar structure with rhythm ratio w. This is a more general case of the self-similar structure, where the length of a branch is proportional with a ratio w to the

Figure 2. Examples of different inflorescence topological structure. The lines in the left of each main axis indicate the profile of the branch lengthes. (a) Constant branch length (Eqn.1); the dashed lines representing the same structures as others; (b) Increasing branch length until a maximum (Eqn.2); (c) Self-similar structure (Eqn.4); (d) Self-similar structure with rhythm ratio w=0.5 (Eqn.5).

distance between the top of its mother axis and the position of the branch, see Fig.2(d).

$$T_2(i) = w \cdot (T_1 - i); T_3(i,j) = w \cdot (T_2(i) - j) \quad (5)$$

Fig.2 illustrates the topology of plants for the four cases mentioned above. It is worth noticing that the topological structure of inflorescence and the form of delay function (see below) can be defined independently as mentioned in [3], although the topological information are used in delay function.

2.2. Quantifying the delay

The growth delay is defined as the time duration between the initiation time t_I (the moment that a phytomer appears), and the expansion time t_E (the moment that the growth of organs is triggered). Time is expressed in cycle, or phyllochron, which is the interval for the creation of a phytomer, generally in terms of growing degree days. While the initiation time of phytomers and the contained organs are given by the organogenesis model, their expansion time is determined by the growth delay. In one phytomer, the growth delay was not necessary the same for all organs, for example, for the case of chrysanthemum, there was no delay for branch leaves. As the basipetal flowering sequence is very common in herbaceous plants, we start by this case to show how the delay function can be defined as a function of coordinate.

A most simple basipetal case is that branches start to grow one after another in each cycle from the top. An illustration is given in Fig.1. In Fig.1, all branch buds keep dormant before the initiation of terminal phytomer of main axis at cycle five ($T_1 = 5$). At cycle 6, the top-most first-order branch is triggered, and then at cycle seven, the expansion of its terminal flower starts as the length of this axis is one. This flower is actually initiated at cycle five, so the delay is two cycles for this flower, indicated in the circle. The other first-order branches, with coordinates (3), (2), (1) respectively, begin to grow sequentially at cycle 7, 8 and 9. The expansion time of a first-order branch of coordinate (i), $t_E(i)$, is then the sum of T_1 and the distance in number of phytomer from its position (i) to length of main stem $(T_1 - i)$. The positional information is converted into delay because one cycle corresponds to the time for initiating a new phytomer. The growth delay $d(i)$ of the bud, being the difference between the expansion time and the initiation time i, can be obtained as $t_E(i) - t_I(i)$ for this simple case. Finally, for a first-order branch of coordinate (i), its initiation time $t_I(i)$, expansion time $t_E(i)$ and delay function $d(i)$ are given as in Eqn.6.

$$\begin{aligned} t_I(i) &= i \\ t_E(i) &= 2T_1 - i \\ d(i) &= t_E(i) - t_I(i) = 2(T_1 - i) \end{aligned} \quad (6)$$

Once an axis starts to grow, phytomers in this axis start expansion in the order that they are created. In other word, they have the same growth delay as indicated in the terminal flower. Therefore, for the terminal phytomer (with a flower) of a branch (i), its expansion time is that of the axis plus the length of the axis.

For a second-order branch of phytomer (i,j), suppose the phyllochron is the same for branches of any order, the initiation time of this phytomer can be computed from its coordinate, as in Eqn.7.

$$t_I(i,j) = i + j \quad (7)$$

The way of computing the expansion time of a second-order branch is similar to the case of the first-order branch. The second-order branch waits until the terminal phytomer of this mother branch (i) has started expansion, which takes place at cycle $t_E(i) + T_2(i)$. As the second-order branches start one by one from the top, it take $(T_2(i) - j)$ cycles for the branch (i,j) to start from that moment. Then the expansion time of branch (i,j) is computed recursively, as shown in Eqn.8.

$$t_E(i,j) = t_E(i) + (2T_2(i) - j) \quad (8)$$

The delay, being the difference between them, is

$$\begin{aligned} d(i,j) &= t_E(i,j) - t_I(i,j) \\ &= 2(T_1 - i) + 2(T_2(i) - j) \\ &= d(i) + 2(T_2(i) - j) \end{aligned} \quad (9)$$

For a third-order branch of coordinate (i,j,k), its initiation time, expansion time and delay function are given directly in recursive way as in Eqns.10, 11, and 12.

$$t_I(i,j,k) = t_I(i,j) + k \tag{10}$$

$$t_E(i,j,k) = t_E(i,j) + (2T_3(i,j) - k) \tag{11}$$

$$d(i,j,k) \quad = \quad d(i,j) + 2(T_3(i,j) - k) \tag{12}$$

The recursive computation can be extended to higher-order branches. In this way, the positional information i, j, k are taken into accounted using the delay function. The result can be seen from the example in Fig.1: of lower position and higher branching order, it takes longer time to have flowering, although these terminal flowers are all initiated at the same cycle.

2.3. General delay functions

The delay functions in Sec.2.2 is limited to the simple basipetal flowering sequence where flowers open in a given speed. Here they are extended to more general functions for the basipetal case, and other flowering sequences are defined.

2.3.1. Basipetal delay functions with delay intensity. Consider the case that the expansion sequence of axillary branch is not necessary one after another. Instead, multiple branches may start simultaneously, followed by the expansion of another cluster of branches. To achieve such effect, instead of having a coefficient of two as in Eqn.9, we use a non-negative vector parameter $\vec{g}$ that reduces or increases the growth delay according to the branching order. Then the delay function for a second-order branch of coordinate (i, j) can be written as in Eqn.13.

$$d(i,j) = g_1 \cdot (T_1 - i) + g_2 \cdot (T_2(i) - j) \tag{13}$$

where g_p is called *delay intensity* of p^{th}-order branch. When the maximum branching order is two, $\vec{g}$ has two components, i.e., $\vec{g} = [\ g_1 \quad g_2\ ]$. Branches have longer dormant stage if the delay intensities are bigger. When $\vec{g} = \vec{0}$, there is no delay, and branches grow immediately at their initiation. Regarding the plant topological structure, the flowering sequence is acropetal for the case of Fig.2(a), while for the case of Fig.2(c), all terminal flowers expand simultaneously. When $\vec{g} = \vec{1}$, all flowers start expansion simultaneously at cycle $T_1^0 + T_2^0 + T_3^0$ for the structure in Fig.2(a), while for Fig.2 (c), the flowers expand one after another. When $\vec{g} = \vec{2}$, for the case of Fig.2(a), branches start extension one by one from top, giving sequential flowering, while the flowering is every two cycles for the case of Fig.2(c), as shown by the example in Fig.1. Obviously, the flowering sequence is dependent on the delay parameters and the topological structure of inflorescence. The same delay function may give different flowering sequence if the plant topology changes.

Real $\vec{g}$ values can give clusters of starting branches because of round-up effect. If several flowers grow simultaneously, they compete for assimilate and share the same life history, finally it is possible to observe groups of flowers of the same size, as seen in chrysanthemum.

The expansion time of a phytomer can finally computed from the delay of the axis that it belongs to. Remind that the initiation time is known according to its coordinate. As the delay function is not necessarily the same for the organs in one phytomer, to distinguish, parameter g_p can be written as g_p^O, O being type of organs, I for internode, F for flower, and L for leave.

2.3.2. Delay intensity dependent on branch position. In real plants, growth delay is not necessary linearly dependent on the position of the branch on the mother axis, as in Eqn. 13. Assuming that the delay intensity increases at lower position of branch, we may introduce such a function as in Eqn.14 for the first and second- order branches.

$$\begin{aligned} g_1 &= g_1^0 \cdot c_1^{T_1 - i} \\ g_2 &= g_2^0 \cdot c_2^{T_2(i) - j} \end{aligned} \tag{14}$$

where g_p^0 is called the *initial delay intensity*, and $c_p (c_p \geq 1)$ is called *position coefficient*. When c_p equals to one, the delay intensity is independent on the position. Otherwise, at lower branch position (smaller i, j values), delay intensities are stronger, and chance is less for these branches to start extension.

2.3.3. Delay intensity dependent on source-sink ratio. Assume that the delay may be regulated by the assimilate competition level within the plant. To simulate such a mechanism, the delay intensity is set to be proportional to the dynamic sink-source ratio. Let $Q(n)$ be the assimilate supply from last cycle $n-1$, $D(n)$ be the total demand for assimilates of the growing organs ay cycle n. Both $Q(n)$ and $D(n)$ can be obtained using different approach, one of them is though calibrating GreenLab functional model [6][9]. The dynamic sink-source ratio is defined as the ratio between the assimilate demand $D(n)$ and supply $Q(n)$. The delay intensity at cycle $n+1$ is then computed as in Eqn.15.

$$g_p(n+1) = g_p^0 + k_p \cdot D(n)/Q(n) \tag{15}$$

In Eqn.15, g_p^0 is the initial delay intensity, and k_p is called *dependency coefficient*, a non-negative value reflecting to which degree the delay intensity is dependent on the sink-source ratio. When k is zero, the delay intensity $\vec{g}$ is constant, as in previous case. Otherwise, according to Eqn.15, when the ratio $Q(n)/D(n)$ decreases, the delay intensity becomes bigger, and hence the delay duration is longer according to Eqn.13. This can limit the expansion of new sink organs and avoid fast increase of plant demand.

In each cycle, the growth delays of dormant branches are recomputed using the updated delay intensity. In this way, the plant become self-regulating system.

2.3.4. Other delay functions. To control the flowering sequence, one can either define the delay function d, or the expansion time t_E. They can be computed from each other as the coordinate gives the initiation time t_I. Here are some flowering patterns with example on second-order branch of coordinate (i, j). These definitions can be extended to other branching orders.

- Divergent flowering sequence. If the flowering sequence is divergent, the expansion function can be defined as in Eqn.16.

$$t_E(i,j) = (T_1 + |\frac{1}{2}T_1 - i|) + (T_2(i) + |\frac{1}{2}T_2(i) - j|) \quad (16)$$

- Constant delay. If all phytomers of a given branching order p have a constant delay d_p^0, independent on its coordinate, the delay function can be written as in Eqn.17.

$$d(i,j) = d_2^0 \quad (17)$$

- Flowering at a given moment. If organs keep dormant until the arrival of a certain event at cycle t^0, such as raining or transition of light cycle, the expansion time of organs can be specified as in Eqn.18.

$$t_E(i,j) = t^0 \quad (18)$$

2.4. Identifying the delay parameters for basipetal case

A relevant issue of a model is to identify parameters according to observed data. We still focus on the basipetal flowering case as it is the most common among herbaceous plants. The aim is to obtain the parameter values of Eqn.13, Eqn.14 or Eqn.15. There are at least two choices. One is to observe the time duration between every two successive branches, but it is tedious to do, and the precision of recorded data is often dependent on the experience of observers. An elegant way is to count the number of visible flowers at different stages, and fit them with the computed number of flowers N_f. In the model, a flower is counted when its age is older than the delay. The numbers of flowers at different stages are functions of the delay parameters and topological parameters. For example, for the self-similar case of $T_2(i) = T_1 - i$, the number of flowers in first-order branches is $N_f(n) = \frac{1}{g_1}(n - T_1), T_1 < n < (g_1 + 1)T_1$, when the delay intensity is constant. For the number of flowers in higher order branches, equations are of more complex form, but it is always possible to count them in simulation software, which is very efficient for herbaceous plants that have a limited number of phytomers. Fig.3 shows

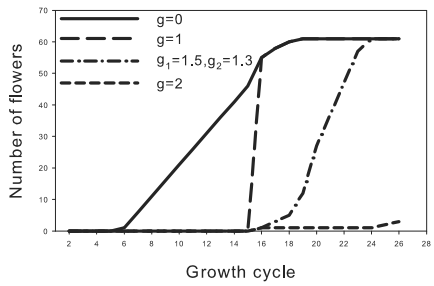

Figure 3. Simulated number of flowers with constant delay intensities (Eqn.13). The plant structure is of type Fig.2 (b), with $T_1 = 15$, $T_2^0 = 5$, $T_3^0 = 3$. The corresponding plant architectures can be seen in Fig.4.

the number of started flowers case of different constant delay intensities, as shown in Fig. 4.

An optimization algorithm is needed in fitting the number of flowers. Because of the round-up effect in computing the number of flower as a function of $\vec{g}$, the model output is generally not sensitive to a small change of parameter values. In that case, gradient-based optimization is not suitable for this purpose. A heuristic algorithm - particle swarm optimization [12] – was chosen for the application.

3. Result

3.1. Simulation

Below we show several simulated virtual plants with inflorescence whose growth is dependent on the delay function. The growth of plant is simulated using GreenLab approach. No delay is set for leaves. The indices of parameter g are indicated only when the values are different for branching orders or organ types. The plant topology is the same for all plants with the maximum branching order being three, of the same type as in Fig.2(b), with $T_1 = 15$, $T_2^0 = 5$, $T_3^0 = 3$.

3.1.1. Effect of delay intensity. The growth delay changes the number of sink organs (internodes and flowers) and consequently the source-sink ratio. As the biomass acquisition of organs is dependent on this source-sink ratio, the organ biomass and size will be changed. Moreover, the delay function changes directly the plant architecture with different number of visible branches. Fig.4 shows the gradient of flowering at the same plant age when parameter g (Eqn.13) takes different values.

From Fig.4 (a) to (e), the growth delay increases with bigger values of parameter g. In case (a) where $g = 0$, branches start growth once they are initiated. This leads to the smallest plant because early competition for assimilates

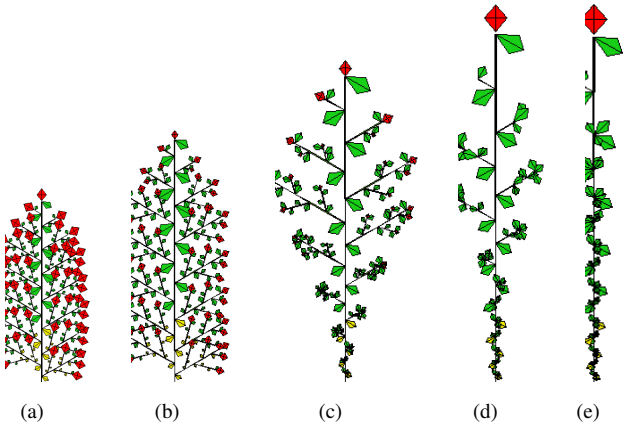

Figure 4. Architectures of inflorescence at cycle 25 using different delay intensities. (a)$g = 0$; (b)$g = 1$; (c)$g_1^F = 1.5, g_2^F = 1.3, g_1^I = 2, g_2^I = 1.3$; (d)$g = 2$; (e)$g = 4$. The plant structure is of type Fig.2 (b), with $T_1 = 15$, $T_2^0 = 5$, $T_3^0 = 3$. Delay intensity g_p (Eqn.13) take the same values for organs and all branching orders if no index is given.

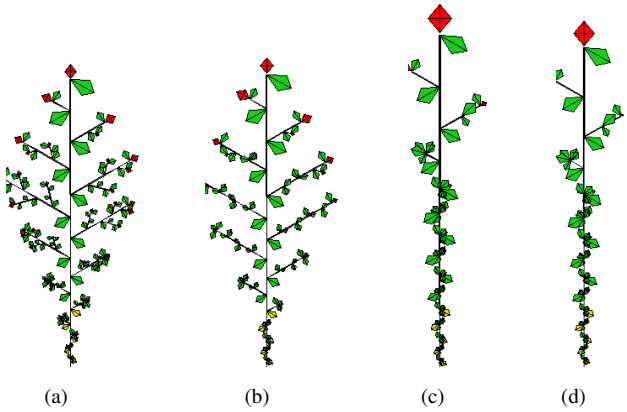

Figure 5. Architectures of inflorescence at cycle 25 with different dependency coefficient $\vec{k}$ on source-sink ratio, according to Eqn.15. (a)$k = 0$; (b)$k = 5$; (c)$k = 50$; (d)$k = 100$. The control plant in (a) is the same as in Fig.4c. Dependency coefficient k_p (Eqn.13) take the same values for all branching orders.

inhibits the expansion of leaves, which are the source organs. Case (b) shows a specific case with $g = 1$, where flowers begin to grow at the same cycle except the top ones. In case (c), a typical basipetal inflorescence structure is found, where flowers locating at higher position gains bigger size because they begin expansion earlier. Different delay parameters for internodes and flowers are set so that the flowers start to grow lightly earlier than the internodes. Expansion of lower branches seem inhibited as the source-sink ratio has been too low. The tallest plants are found in cases (d) and (e), as there is little competition from the branches on the extension of main stem.

3.1.2. Effect of source-sink ratio Q/D. Consider the case where the values of parameter g depend on the source-sink ratio, as in Eqn.15. The Q/D ratio typically increases with plant age in vegetative stage until a maximum value, and decreases afterwards [6] since expansion of flowers increases the plant demand D and possible senescence of leaves can decrease the assimilate supply Q. Therefore, stronger dependency on the ratio Q/D will lead to bigger delay intensities and therefore less flowers. Fig.5 shows the effect of assimilate supply and demand ratio on the plant architecture with different dependency coefficient k.

Increasing dependency on Q/D from Fig.5 (a) to (d) leads to more delay. Compared to the control plant in the case (a), the plant in (b) has less second-order branches. In case (c), the first-order branches have shrunk. In case (d), only few branches in top of plants expanded, typically observed in nature. Comparing the Fig.5 (d) and Fig.4, it can be seen sink-source dependent delay intensity give different plant

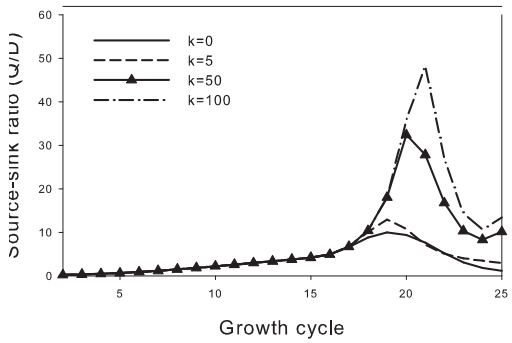

Figure 6. Simulated source-sink ratio (Q/D) with different dependency coefficient k of delay parameters on Q/D, using the same parameter sets as in Fig.5.

shape.

As the delay of flower expansion influences on the plant demand, there is actually feedback of the growth delay on the source-sink ratio. Fig.6 shows the source-sink ratio at different dependency coefficient k on Q/D ratio. From the figure it can be seen that Q/D values increase in vegetative stages, and decrease at flowering stage. At higher k, as delay is greater, and less flowers begin to grow, plant demand is smaller, leading to higher Q/D. At later stage, the dynamics of Q/D ratio highly depends on the leaf functioning time. In this example, leaf functioning time is 20, and at plant age 25, all leaves are still contributing to biomass production.

3.1.3. Effect of environmental condition. The environmental conditions can influence on the resource supply for

plant growth. In case that the growth delay is dependent on sink-source ratio, the adaption of plant architecture to environment, or plant plasticity, can be partially simulated. In GreenLab model, a variable E is used for indicating environmental conditions at each cycle. The biomass supply at each cycle $Q(n)$ is proportional to E. The meaning of E can be either the intercepted light integral per cycle, or the potential evapo-transpiration, if water is the limiting factor. In previous examples as in Fig.4 and 5, E is set to be one. Fig.7 shows the simulated plant architectures when the control parameter E changes, where k equal to 50, and delay parameters depend on the source-sink ratio.

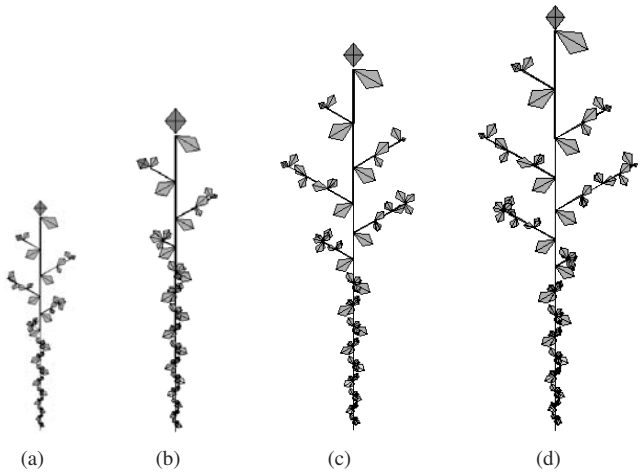

Figure 7. Architectures of inflorescence dependent on environmental factor E. (a)$E = 0.5$; (b)$E = 1$; (c)$E = 1.5$; (d)$E = 2$. The control plant in (b) is the same as in Fig.5c.

From Fig.7 it can be seen that when E increases, the plant height increases with E. It is worthy to notice that the architectures are not simply amplified at better environmental condition. Instead, more branches start extending at better condition.

3.2. Applications

To simulate the development and growth process of a herbaceous plant with basipetal inflorescence, the three components of the model as introduced in Sec.2 need to be calibrated. Generally the parameters of the organogenesis model can be observed directly from the plant architecture with naked eyes, which are the length of branches of different types, *i.e.*, T_1, $T_2(i)$, $T_3(i,i)$, *etc*. The parameters of delay function can be identified using the inverse method as in Sec.2.4. After that, parameters controlling the functional model can be identified as the last step by fitting the organ biomass.

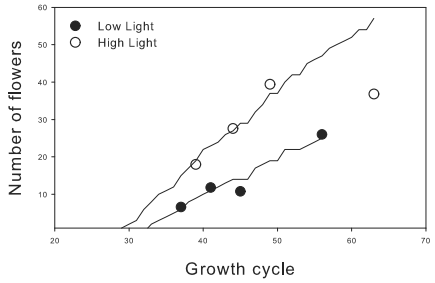

Figure 8. The number of flowers in chrysanthemum plants in generative stage, from four samplings (circles) and model output (lines), at low and high light level.

An application is made on chrysanthemum using GreenLab approach. The number of flowers were counted at four stages from flowering (unpublished data). They were the fitting target in identifying the delay parameters. The results of fitting for two light levels are shown in Fig.8. Remember that before the calibration of the functional model, the source-sink ratio is still unknown, therefore only positional information can be used to simulate the change of growth delay intensity (14). Four parameters (g_1^0, g_2^0, c_1, c_2) were identified in this fitting exercise.

The next step is the identification of source-sink parameters by fitting simultaneously the biomass of different types of organs (main stem leaves, branch leaves, main stem internodes, branch internodes, flowers) from nine sampling stages. The delay function is used in the functional model to compute the plant demand. The model gives good fitting on all data with a set of parameters regulating biomass production and repartition (unpublished data). Fig.9 shows two virtual chrysanthemums grown at low and high light conditions, with organ size and weight being computed using the calibrated model. At high light condition, the simulated plants produce more flowers, while the size of flowers is equivalent to the low light condition. This result is close to the behavior of real plants, which is assured by the delay function.

4. Conclusions and perspectives

In this paper we presented the delay functions controlling various flowering sequence in herbaceous plants with inflorescence. Emphasis was made on the basipetal flowering which is very common in crops. The effect of different delay parameters on plant growth was visualized by the plant architectures. Especially, it was presented how the growth delay and consequently the plant architecture can be adjusted by the internal source-sink ratio of plant and furthermore the environmental level. Simulation results in Fig.5 reproduced faithfully the apical dominance effect. An

(a) (b)

Figure 9. Simulated cut chrysanthemums under (a)low light and (b)high light levels.

example of application was given on chrysanthemum to illustrate the calibration of the delay function (Fig.8) and the importance of delay function in describing the plant growth.

Differing from the previous works [1] [3] where flowering sequence was controlled purely by the plant development, in the current work, the flowering sequence was controlled by the delay functions, which quantifies the time duration from organ initiation and organ expansion. Finally the resulting flowering sequence is dependent both on the delay function and the topological structures of plant, which result from the organ initiation sequences. Moreover, from the computer simulation point of view, the computation of delay with equations is more efficient compare to the step by step simulation of signal propagation in the plant structure.

It is often controversial whether it is hormone or source-sink ratio that control flowering. Lindenmayer [3] has proposed two mechanisms control the flowering sequence: (1) the florigen (the flowering substances, which have unfortunately not been identified despite of more than 70 years' effort) propagates from the base of plant to main stem and branches. After the arrival of florigen, the apex is rapidly transformed from a vegetative to a flowering condition; (2) the production of an inhibitory hormone (auxin) by the main apices and its basipetal transport in the branches (role of apical dominance). The first mechanism corresponds to the organogenesis model in this paper. The simulated result as in Fig.5 demonstrated that based on a source-sink approach, the effect of inhibitory hormone can be well simulated. In future, it is encouraging to test the link between the growth delay and source-sink ratio on different species and different environmental conditions.

Acknowledgment

This study is supported by National 863 High-Tech Research Plan of China (No. 2008AA10Z218, No. 2006AA10Z229), NSFC (No. 60703043), the Excellent SKL Project of NSFC (No.60723005) and China Postdoctoral Special Foundation (Grant No. 200801127). We thank Prof. BaoGui Zhang from CAU for checking on the manuscript.

References

[1] P. Prusinkiewicz, A. Lindenmayer, and J. Hanan, "Developmental models of herbaceous plants for computer imagery purposes," *Computer graphics*, vol. 22, pp. 141–150, 1988.

[2] X. Zhao, F.-L. Xiong, B.-g. Hu, P. de Reffye, and M.-Z. Kang, "Simulation of plant inflorescence based on dual-scale automaton," *Chinese Journal of Computers*, vol. 26, no. 1, pp. 116–124, 2003.

[3] A. Lindenmayer, *Positional controls in plant development*. Cambridge University Press, 1984, ch. Position and temporal control mechanisms in inflorescence development, pp. 461–486.

[4] J. Long and M. Kathryn Barton, "Initiation of axillary and floral meristems in arabidopsis," *Developmental Biology*, vol. 218, pp. 341–353, 2000.

[5] M.-Z. Kang, E. Heuvelink, and P. de Reffye, "Building virtual chrysanthemum based on sink source relationships: preliminary results," in *Acta Horticulturae*, L. Marcelis, G. van Straten, C. Stanghellini, and E. Heuvelink, Eds., vol. 718, Wageningen, Netherlands, 2006, pp. 129–136.

[6] A. Christophe, V. Letort, I. Hummel, P.-H. Cournède, P. de Reffye, and J. Lecoeur, "A model-based analysis of the dynamics of carbon balance at the whole-plant level in arabidopsis thaliana," *Functional Plant Biology*, vol. 35, pp. 1147–1162, 2008.

[7] S. Carvalho and E. Heuvelink, "Effect of assimilate availability on flower characteristics and plant height of cut chrysanthemum: an integrated study," *Journal of Horticultural Science and Biotechnology*, vol. 78, pp. 711–720, 2003.

[8] J. Vos, L. Marcelis, P. de Visser, and P. Struik, Eds., *Functional-structural plant modelling in crop production*. Kluwer Academic Publishers, 2007.

[9] Y. Guo, Y.-T. Ma, Z.-G. Zhan, B.-G. Li, M. Dingkuhn, D. Luque, and P. de Reffye, "Parameter optimization and field validation of the functional-structural model greenlab for maize," *Annals of Botany*, vol. 97, pp. 217–230, 2006.

[10] Q.-X. Dong, G. Louarn, Y.-M. Wang, J.-F. Barczi, P. de Reffye, and 2008, "Does the structurecfunction model greenlab deal with crop phenotypic plasticity induced by plant spacing? a case study on tomato," *Annals of Botany*, vol. 101, pp. 1195–1206, 2008.

[11] M. Allen, P. Prusinkiewicz, and T. DeJong, "Using l-systems for modeling source-sink interactions, architecture and physiology of growing trees: the l-peach model," *New Phytologist*, vol. 166, pp. 869–880, 2005.

[12] S. He, Q.-H. Wu, J.-Y. Wen, J.-R. Saunders, and R. Paton, "A particle swarm optimizer with passive congregation," *BioSystems*, vol. 78, pp. 135–147, 2004.